Journal of Electroanalytical Chemistry 638 (2010) 100–108

Contents lists available at ScienceDirect

Journal of Electroanalytical Chemistry

journal homepage: www.elsevier.com/locate/jelechem

Electrochemical reduction of 5-chloro-2-(2,4-dichlorophenoxy)phenol (triclosan) in dimethylformamide

Kyle N. Knust [a], Matthew P. Foley [a], Mohammad S. Mubarak [b], Sonja Skljarevski [a], Krishnan Raghavachari [a], Dennis G. Peters [a,*]

[a] Department of Chemistry, Indiana University, Bloomington, IN 47405, USA
[b] Department of Chemistry, The University of Jordan, Amman 11942, Jordan

ARTICLE INFO

Article history:
Received 30 July 2009
Received in revised form 5 October 2009
Accepted 7 October 2009
Available online 25 October 2009

Keywords:
Triclosan
5-Chloro-2-(2,4-dichlorophenoxy)phenol
Catalytic reduction
Nickel(I) complexes

ABSTRACT

Cyclic voltammetry and controlled-potential (bulk) electrolysis have been used to investigate the direct reduction of 5-chloro-2-(2,4-dichlorophenoxy)phenol (triclosan, **1**) in dimethylformamide (DMF) containing tetra-*n*-butylammonium tetrafluoroborate ($TBABF_4$). Cyclic voltammograms for reduction of **1** at glassy carbon electrodes exhibit three irreversible peaks attributed to successive reductive cleavage of the three aryl carbon–chlorine bonds. Bulk electrolyses of **1** at reticulated vitreous carbon cathodes held at a potential between the first and second cathodic peaks afford only 5-chloro-2-(4-chlorophenoxy)phenol; however, at a more negative potential, a mixture of 5-chloro-2-(4-chlorophenoxy)phenol, 5-chloro-2-phenoxyphenol, and 2-phenoxyphenol is obtained. A scheme consisting of electron-transfer steps and accompanying chemical reactions is proposed that follows the classic mechanism for the reduction of aryl halides. To provide support for this mechanism, theoretical calculations based on density functional theory have been performed to model the electronic structures of **1** and the likely intermediates formed via its electroreduction. Catalytic reduction of **1** by nickel(I) salen and nickel(I) diethylsalen, each mediator electrogenerated at a glassy carbon electrode in DMF – 0.10 M $TBABF_4$, has been explored with the aid of cyclic voltammetry and controlled-potential electrolysis.

1. Introduction

First used in 1972 as a component of surgical scrub for aseptic hospital procedures, triclosan or 5-chloro-2-(2,4-dichlorophenoxy)phenol (**1**) is a pervasive, broad-spectrum antibacterial disinfectant found in a number of common household products, including cosmetics, deodorants, mouthwashes, soaps, and toothpastes, and it is infused in consumer items such as bedding, kitchen utensils, socks, toys, and trash bags.

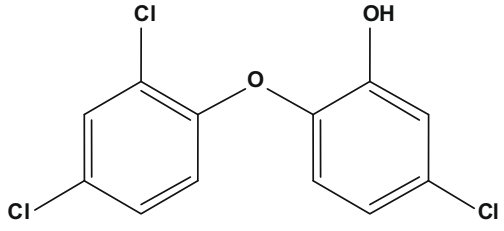

1

There have been reports that exposure to triclosan causes skin irritation, photoallergic contact dermatitis, and immunotoxic and neurotoxic reactions in humans. Substantial levels of triclosan have been found in human milk and fatty tissues. Furthermore, the Environmental Protection Agency of the United States has indicated that carcinogenic dioxins might arise as an impurity in the manufacture of triclosan, and it has been found that dioxins can be formed when triclosan-contaminated natural waters are exposed to sunlight. Accordingly, there is interest in the degradative dechlorination of triclosan.

Over the past decade, there has been a number of publications [1–11] pertaining to the electrochemical behavior of triclosan. Pemberton and Hart [1] used a screen-printed carbon electrode for the analytical determination of triclosan in toothpastes and mouthwashes; in an aqueous medium at pH 10, electrooxidation of triclosan gives a single wave that involves a one-electron transfer. Safavi et al. [2,3] investigated the electrochemical behavior of triclosan at mercury cathodes. Using cyclic voltammetry and controlled-potential electrolysis, Wang and co-workers [4] investigated the direct reduction of triclosan at carbon cathodes in aqueous buffer solutions and in methanol or dimethylformamide containing tetra-*n*-butylammonium hydroxide; two products, chlorobenzene and 2-phenoxyphenol, were identified. Two papers

* Corresponding author. Tel.: +1 812 855 9671; fax: +1 812 855 8300.
E-mail address: peters@indiana.edu (D.G. Peters).

0022-0728/$ - see front matter © 2009 Elsevier B.V. All rights reserved.
doi:10.1016/j.jelechem.2009.10.012

[5,6] have dealt with the oxidation of triclosan at boron-doped diamond surfaces. A surfactant-coated electrode has been evaluated by Raghupathy and co-workers [7] for the oxidative detection of triclosan in aqueous media. Sirés et al. [8] examined the electro-Fenton oxidation of triclosan in an aqueous medium of pH 3 and in an acetonitrile–water mixture; in the latter solvent, mixtures of 2,4-dichlorophenol, 4-chlorocatechol, chlorohydroquinone, chloro-*p*-benzoquinone, and carboxylic acids (such as maleic, oxalic, formic, and acetic acid) were obtained. Strategies have been reported for the oxidative measurement of triclosan in an aqueous medium at an indium-doped tin oxide electrode coated with a film composed of carbon nanoparticles and poly(diallyldimethylammonium chloride) (PDDAC) [9] and at a glassy carbon electrode with a cellulose film embedded with PDDAC [10]. Cyclic voltammograms for the oxidation of triclosan adsorbed onto carbon nanoparticles immobilized on a glassy carbon surface exhibit a single peak attributed to a one-electron process to form a phenoxy radical that undergoes polymerization [11].

During the same period of time as the preceding references, there have been papers [12–17] dealing with the electrochemical degradation of chlorinated phenols. As part of an analytical detection protocol, Saby and co-workers [12] have investigated the electrocatalytic oxidation of mono-, di-, tri-, tetra-, and pentachlorophenols, and Rodgers et al. [13] have employed PbO_2, IrO_2, and SnO_2 anodes in an aqueous medium to dechlorinate a similar set of compounds. Cyclic voltammetry has been used by Ežerskis and Jusys [14] to probe the oxidation of chlorinated phenols at platinum and gold electrodes in aqueous sodium hydroxide solutions, and Cheng and co-workers [15,16] utilized a variety of cathode materials to study the hydrodehalogenation of chlorinated phenols. Finally, in a very recent report, Wang and Wang [17] have examined the electrochemical degradation of 2,4-dichlorophenol in a diaphragm cell consisting of a palladium-modified gas-diffusion cathode, a titanium–iridium oxide–ruthenium oxide anode, and an aqueous sodium sulfate electrolyte solution; although the primary products are 4-chlorophenol, 2-chlorophenol, and phenol, these species are subsequently converted into a mixture of other compounds (hydroquinone, benzoquinone, and aliphatic carboxylic acids).

As part of an ongoing program in our laboratory, we have already studied the direct and cobalt(I) salen-catalyzed electrochemical dechlorination of several environmentally deleterious substances—1,1,2-trichloro-1,2,2-trifluoroethane (CFC-113) [18], 4,4′-(2,2,2-trichloroethane-1,1-diyl)bis(chlorobenzene) (DDT) [19,20], 1,1,1-trichloro-2,2,2-trifluoroethane (CFC-113a) [21], and hexa- and pentachlorobenzene [22]. In the present investigation, we have used cyclic voltammetry and controlled-potential electrolysis with glassy carbon cathodes to examine the direct as well as the nickel(I) salen- and nickel(I) diethylsalen-catalyzed reduction of triclosan in dimethylformamide containing 0.10 M tetra-*n*-butylammonium tetrafluoroborate. Gas chromatography and gas chromatography–mass spectrometry have been employed to separate, identify, and quantitate the electrolysis products. A mechanistic scheme, invoking the intermediacy of carbanions, is proposed to account for the formation of the various products. Theoretical calculations, based on density functional theory, are in support of our mechanistic picture, and hint that a novel intramolecular proton-transfer reaction might be involved in a product-forming channel.

2. Experimental

2.1. Reagents

Triclosan [5-chloro-2-(2,4-dichlorophenoxy)phenol] was purchased in 99% purity from Alfa Aesar; 3-phenoxyphenol (99%), used as a standard for the quantitation of 2-phenoxyphenol, was acquired from Acros Organics. Each of the following chemicals, used without additional purification, was obtained from the Aldrich Chemical Company: *n*-hexadecane (99%), 4-chloro-2-methoxyphenol (technical grade), copper(II) carbonate (basic, reagent grade), 1-bromo-4-chlorobenzene (99%), bromobenzene (99%), aluminum chloride (anhydrous powder, 99.99%), ethylenediamine (99+%), 1-(2-hydroxyphenyl)propan-1-one (97%), nickel(II) acetate tetrahydrate (98%), and [[2,2′-[1,2-ethanediylbis(nitrilomethylidyne)]bis[phenolato]]-*N*,*N*′,*O*,*O*′]nickel(II) (hereafter referred to as nickel(II) salen, 98%). Dimethylformamide (DMF, ACS grade, 99.8%) from Fisher Scientific was utilized without further purification as the solvent for all electrochemical experiments. Tetra-*n*-butylammonium tetrafluoroborate ($TBABF_4$, >98%), from GFS Chemicals, Inc., was employed as supporting electrolyte and was stored in a vacuum oven at 70–80 °C to remove traces of water present. All deaeration procedures were accomplished with zero-grade argon (Air Products).

2.2. Cells, electrodes, instrumentation, and procedures

Information concerning the cell for cyclic voltammetry is available in an earlier paper [23]. We constructed a circular, planar working electrode with an area of 0.071 cm^2 for cyclic voltammetry by press-fitting a short length of glassy carbon rod (Grade GC-20, 3.0-mm-diameter, Tokai Electrode Manufacturing Company, Tokyo, Japan) into a Kel-F shroud. Before each cyclic voltammogram was recorded, the working electrode was cleaned with an aqueous suspension of 0.05-μm alumina on a Master-Tex (Buehler) polishing pad, after which the electrode was rinsed ultrasonically in DMF and wiped dry before being inserted into the electrochemical cell. To acquire cyclic voltammograms, we employed a Faraday MP scanning potentiostat (model F02A, Obbligato Objectives Inc.) together with a companion program installed on a personal computer.

Details pertaining to the cell, instrumentation, and procedure for controlled-potential electrolysis are presented in a previous publication [24]. Working electrodes for controlled-potential electrolysis were reticulated vitreous carbon disks (approximately 4 mm in thickness, 2.4 cm in diameter, and 200 cm^2 in surface area) that were cut from commercially available material (RVC 2X1-100S, Energy Research and Generation, Inc., Oakland, CA). Procedures used to fabricate, clean, and handle these disks are described more fully in the literature [25].

All potentials in this report are quoted with respect to a reference electrode consisting of a cadmium-saturated mercury amalgam in contact with DMF saturated with both cadmium chloride and sodium chloride; this electrode has a potential of −0.76 V versus the aqueous saturated calomel electrode (SCE) at 25 °C [26–28].

2.3. Separation, identification, and quantitation of products

Two different approaches were taken to quantitate the various products after each controlled-potential electrolysis. For the first procedure, the catholyte was dissolved in diethyl ether and partitioned three times between ether and brine; then the ether phase was dried over anhydrous sodium sulfate and concentrated with the aid of rotary evaporation. However, we discovered that this method led to the loss of products into the aqueous phase. Thus, we adopted a second and better procedure that involved dilution of the catholyte with a ninefold volume excess of methanol, followed by direct analysis of an aliquot of this mixture. Products were identified by means of gas chromatography–mass spectrometry (GC–MS); for this purpose, we used a Hewlett–Packard 6890 N gas chromatograph, fitted with a 30 m × 0.25 mm DB-5MS capil-

lary column (Agilent Corporation) and coupled to a Hewlett–Packard 5973 inert mass-selective detector. We confirmed 5-chloro-2-(4-chlorophenoxy)phenol and 5-chloro-2-phenoxyphenol as electrolysis products by comparing their gas chromatographic retention times and mass spectra with those of authentic samples synthesized as described below; high-resolution mass spectral data were acquired with the aid of a Thermo Electron Corporation MAT 95XP-Trap instrument. A minor electrolysis product, 2-phenoxyphenol, was identified from GC–MS data: *m*/*z* (70 eV): 186 $[M]^+$ (100%); 157 $[M–C_2H_5]^+$ (10%); 129 $[M–C_4H_9]^+$ (7%); 109 $[C_6H_5O_2]^+$ (6%); 77 $[C_6H_5]^+$ (14%). In addition, the presence of tri-*n*-butylamine (formed as a by-product via the Hofmann elimination involving electrogenerated carbanionic intermediates and the tetra-*n*-butylammonium cation of the supporting electrolyte) was verified on the basis of GC–MS measurements.

Quantitation of all products was done with an Agilent 7890A gas chromatograph equipped with a flame-ionization detector and a 30 m × 0.25 mm capillary column (J & W Scientific) with a DB-5 stationary phase consisting of 5% phenylpolysiloxane and 95% methylpolysiloxane. Integration of peak areas was accomplished with ChemStation software, and an Excel spreadsheet was used to determine the percentage of each product. A known quantity of a nonvolatile, electroinactive internal standard (*n*-hexadecane) was added to each solution prior to an electrolysis. All product yields reported in this paper denote the absolute percentage of starting material incorporated into each species. A full description of the protocol employed for the determination of gas chromatographic response factors and for the quantitation of products is given elsewhere [29].

2.4. Synthesis of 4-chloro-1-(4-chlorophenoxy)-2-methoxybenzene

We prepared 4-chloro-1-(4-chlorophenoxy)-2-methoxybenzene via a modified version of a procedure patented by Di Teodoro et al. [30]. Our protocol involved introducing 4-chloro-2-methoxyphenol (3.45 mL, 28.4 mmol) and *m*-xylene (4.45 mL, 36.4 mmol) into a 25-mL round-bottom flask fitted with a Dean–Stark trap and a reflux condenser, and heating the mixture to 80 °C with constant stirring followed by addition of potassium hydroxide (0.6 g, 11 mmol). After being heated at 145 °C for 2 h, the mixture was cooled to 100 °C and copper(II) carbonate (0.0159 g, 71.9 μmol) and 1-bromo-4-chlorobenzene (4.59 g, 24.0 mmol) were added to the flask, and the mixture was reheated at 145 °C for 2.5 h. Upon being cooled to room temperature, the product mixture was filtered to remove insoluble potassium salts, and the remaining solution was partitioned twice between 0.1 M sodium hydroxide solution and diethyl ether to remove unreacted 4-chloro-2-methoxyphenol. Then the ether extracts were combined, washed twice with distilled water, and dried over anhydrous sodium sulfate, and the ether was removed under reduced pressure. Simple distillation of the residue was used to remove *m*-xylene. Finally, the product was purified by passage through a silica-gel column, with hexane and then hexane–ethyl acetate (1:1) as eluents, to afford the desired 4-chloro-1-(4-chlorophenoxy)-2-methoxybenzene; mass spectral data were as follows: *m*/*z* (70 eV): 272 $[M]^+$ (11%); 270 $[M]^+$ (65%); 268 $[M]^+$ (100%); 220 $[M–Cl–CH_3]^+$ (25%); 218 $[M–Cl–CH_3]^+$ (75%); 113 $[C_6H_4{}^{37}Cl]^+$ (3%); 111 $[C_6H_4{}^{35}Cl]^+$ (9%); HRMS *m*/*z*: calcd. for $C_{13}H_{10}O_2{}^{35}Cl_2$ $[M]^+$ 268.0058, found 268.0046; calcd. for $C_{13}H_{10}O_2{}^{35}Cl{}^{37}Cl$ $[M]^+$ 270.0028, found 270.0027; calcd. for $C_{13}H_{10}O_2{}^{37}Cl_2$ $[M]^+$ 271.9999, found 272.0012.

2.5. Synthesis of 5-chloro-2-(4-chlorophenoxy)phenol

We prepared 5-chloro-2-(4-chlorophenoxy)phenol by means of a previously published procedure [30] that involves addition of petroleum ether (45 mL) and anhydrous aluminum chloride (0.90 g, 6.75 mmol) to 4-chloro-1-(4-chlorophenoxy)-2-methoxybenzene (0.84 g, 3.12 mmol) in a 100-mL round-bottom flask fitted with a reflux condenser. After the mixture was refluxed at 75–85 °C for 1 h, hydrochloric acid (2.0 M, 50 mL) was added at 70 °C and the mixture was stirred for an additional 15 min. Then the organic layer was washed with water and dried over anhydrous sodium sulfate, and the solvent was removed under reduced pressure to afford the desired product in approximately 95% purity, as indicated by gas chromatography–mass spectrometry: *m*/*z* (70 eV): 258 $[M]^+$ (11%); 256 $[M]^+$ (64%); 254 $[M]^+$ (100%); 220 $[M–H–Cl]^+$ (3%); 218 $[M–H–Cl]^+$ (7%); 184 $[M–2Cl]^+$ (9%); 145 $[C_6H_4O_2{}^{37}Cl]^+$ (4%); 143 $[C_6H_4O_2{}^{35}Cl]^+$ (12%); HRMS *m*/*z*: calcd. for $C_{12}H_8O_2{}^{35}Cl_2$ $[M]^+$ 253.9901, found 253.9888; calcd. for $C_{12}H_8O_2{}^{35}Cl{}^{37}Cl$ $[M]^+$ 255.9872, found 255.9861; calcd. for $C_{12}H_8O_2{}^{37}Cl_2$ $[M]^+$ 257.9842, found 257.9831.

2.6. Synthesis of 4-chloro-2-methoxy-1-phenoxybenzene

To prepare 4-chloro-2-methoxy-1-phenoxybenzene, we used the procedure described in Section 2.4 for the synthesis of 4-chloro-1-(4-chlorophenoxy)-2-methoxybenzene, except that bromobenzene (3.77 g, 24.0 mmol) was used instead of 1-bromo-4-chlorobenzene. We confirmed the identity of the product with the aid of gas chromatography–mass spectrometry: *m*/*z* (70 eV): 236 $[M]^+$ (34%); 234 $[M]^+$ (100%); 221 $[M–CH_3]^+$ (1%); 219 $[M–CH_3]^+$ (5%); 205 $[M–OCH_3]^+$ (1%); 203 $[M–OCH_3]^+$ (2%); 184 $[M–Cl–CH_3]^+$ (32%); 77 $[C_6H_5]^+$ (17%); HRMS *m*/*z*: calcd. for $C_{13}H_{11}O_2{}^{35}Cl$ $[M]^+$ 234.0448, found 234.0440; calcd. for $C_{13}H_{11}O_2{}^{37}Cl$ $[M]^+$ 236.0418, found 236.0431.

2.7. Synthesis of 5-chloro-2-phenoxyphenol

For the synthesis of 5-chloro-2-phenoxyphenol, the procedure outlined in Section 2.5 for the preparation of 5-chloro-2-(4-chlorophenoxy)phenol was employed, except that 4-chloro-2-methoxy-1-phenoxybenzene (0.64 g, 3.12 mmol) was substituted for 4-chloro-1-(4-chlorophenoxy)-2-methoxybenzene. We obtained the desired product in approximately 97% purity, as indicated by gas chromatography–mass spectrometry: *m*/*z* (70 eV): 222 $[M]^+$ (33%); 220 $[M]^+$ (100%); 203 $[M–OH]^+$ (2%); 184 $[M–H–Cl]^+$ (4%); 145 $[C_6H_4O_2{}^{37}Cl]^+$ (3%); 143 $[C_6H_4O_2{}^{35}Cl]^+$ (10%); 77 $[C_6H_5]^+$ (23%); HRMS *m*/*z*: calcd. for $C_{12}H_9O_2{}^{35}Cl$ $[M]^+$ 220.0291, found 220.0288; calcd. for $C_{12}H_9O_2{}^{37}Cl$ $[M]^+$ 222.0262, found 222.0263.

2.8. Synthesis of [[2,2′-[1,2-ethanediylbis(nitrilopropylidyne)]-bis[phenolato]]-N,N′,O,O′]nickel(II) (nickel(II) diethylsalen)

Our synthesis of nickel(II) diethylsalen was patterned after a procedure outlined by Gosden et al. [31]. For the preparation of the ligand, ethylenediamine was added to a stirred solution of 1-(2-hydroxyphenyl)propan-1-one dissolved in ethanol; the diamine-to-ketone molar ratio was 2:1. After the addition, the reaction mixture was heated to reflux for a minimum of 30 min. When the solution was allowed to cool to room temperature, a bright yellow solid precipitated, which was collected by cold suction filtration, washed with cold ethanol to remove excess starting materials, and dried in air. Its identity was confirmed with the aid of electrospray ionization–mass spectrometry [32] and ^{1}H NMR spectroscopy (300-MHz Varian Gemini 2000 instrument): *m*/*z* (70 eV): 325 $[M + H]^+$; ^{1}H NMR ($CDCl_3$): δ 7.52–6.70 (8H), 3.98 (s, $–CH_2–N{=}C–$, 4H), 2.82 (q, $CH_3–C\mathbf{H_2}–C{=}N–$, 4H), 2.82 (t, $C\mathbf{H_3}–CH_2–$, 6H); the hydroxyl protons of the ligand were not detected due to exchange with traces of water present in the $CDCl_3$.

Metallation of the ligand to form the desired complex was accomplished by addition of a stoichiometric amount of nickel(II) acetate tetrahydrate in water to an ethanolic solution of the ligand.

Upon introduction of the nickel(II) salt, the color of the solution changed from bright yellow to red as nickel(II) was chelated by the ligand. Crystals were collected by cold vacuum filtration, washed with cold ethanol, and air dried. High-resolution mass spectrometry (HRMS) was used to verify the identity of the nickel(II) complex; *m*/*z*: calcd. for $C_{20}H_{22}N_2O_2{}^{58}Ni$ $[M]^+$ 380.1035, found 380.1026; calcd. for $C_{20}H_{22}N_2O_2{}^{60}Ni$ $[M]^+$ 382.0989, found 382.0996; calcd. for $C_{20}H_{22}N_2O_2{}^{61}Ni$ $[M]^+$ 383.0992, found 383.1021; calcd. for $C_{20}H_{22}N_2O_2{}^{62}Ni$ $[M]^+$ 384.0965, found 384.1001; calcd. for $C_{20}H_{22}N_2O_2{}^{64}Ni$ $[M]^+$ 386.0961, found 386.1000.

3. Results and discussion

3.1. Cyclic voltammetric behavior of triclosan and its reduction products

Shown in Fig. 1, curve A, is a cyclic voltammogram recorded with a freshly polished glassy carbon electrode at 100 mV s^{-1} for the reduction of a 5.0 mM solution of triclosan in oxygen-free DMF containing 0.10 M $TBABF_4$. Three irreversible cathodic waves are observed, having peak potentials of −1.57, −1.76, and −2.05 V, which presumably correspond to the consecutive reductive cleavage of each of the three aryl carbon–chlorine bonds. However, the relative heights of these three peaks are different, and the first peak is unusually broad. In contrast to the behavior of triclosan observed in the present investigation, Wang and co-workers [4] reported that reduction of triclosan at a carbon fiber electrode gives a single cathodic peak in Britton-Robinson buffers of pH < 8, whereas two cathodic peaks are seen in aqueous media of pH > 8 and in a methanol – 0.10 M $NaClO_4$ solution of pH 6.3.

A cyclic voltammogram recorded at 100 mV s^{-1} for the reduction of a 5.0 mM solution of 5-chloro-2-(4-chlorophenoxy)phenol (a major product of the bulk electrolysis of triclosan) in oxygen-free DMF – 0.10 M $TBABF_4$ at a freshly polished glassy carbon electrode is depicted in Fig. 1, curve B. Two irreversible waves, with peak potentials of −1.77 and −2.03 V, are seen. We conclude that these two peaks, attributed to the sequential scission of each of the carbon–chlorine bonds, correspond to the second and third peaks of curve A.

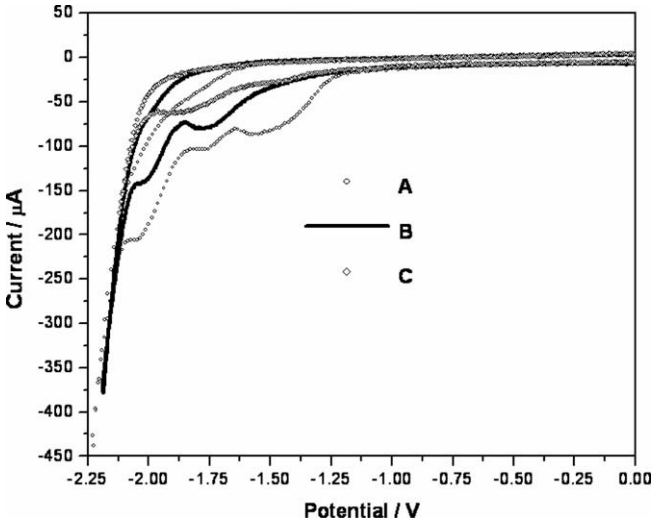

Fig. 1. Cyclic voltammograms recorded at a scan rate of 100 mV s^{-1} with a freshly polished glassy carbon electrode (area = 0.071 cm^2) in oxygen-free DMF containing 0.10 M $TBABF_4$: (A) 5.0 mM triclosan; (B) 5.0 mM 5-chloro-2-(4-chlorophenoxy)phenol; (C) 5.0 mM 5-chloro-2-phenoxyphenol. All scans go from 0 to −2.25 to 0 V.

In curve C of Fig. 1 is a cyclic voltammogram for the reduction of 5.0 mM 5-chloro-2-phenoxyphenol obtained at 100 mV s^{-1} in oxygen-free DMF – 0.10 M $TBABF_4$ at a freshly polished glassy carbon electrode. Inexplicably, but very reproducibly, the reduction of 5-chloro-2-phenoxyphenol gives rise to two irreversible peaks at −1.46 and −1.88 V. What is also unexpected is that the peak potentials for reduction of 5-chloro-2-phenoxyphenol are significantly more positive than those predicted on the basis of a cyclic voltammogram for either triclosan (Fig. 1, curve A) or 5-chloro-2-(4-chlorophenoxy)phenol (Fig. 1, curve B). So far, we have not been able to account for this behavior, but additional research is in progress concerning these findings.

We questioned whether 2-phenoxyphenol, resulting from the complete reductive dechlorination of triclosan, might contribute to the electrochemical response seen in curves A–C in Fig. 1. Some years ago, using cyclic voltammetry and controlled-potential electrolysis, Bartak and co-workers [33,34] found that 1-isocyano-4-phenoxybenzene (4-cyanodiphenyl ether, E_{pc} = −1.59 V), 2-phenoxybenzonitrile (2-cyanodiphenyl ether, E_{pc} = −1.46 V), and oxydibenzene (diphenyl ether, E_{pc} = −2.19 V) undergo reduction at platinum cathodes in DMF containing 0.10 M tetra-*n*-butylammonium perchlorate. Electrogenerated radical–anions of 1-isocyano-4-phenoxybenzene undergo irreversible coupling to give dimeric dianions, each of which loses a phenoxide ion to form other species, at least one of which is reducible. Radical–anions arising from 2-phenoxybenzonitrile can couple to yield three different dimeric dianions, one of which expels phenoxide ion to produce a monoanion. On the other hand, when oxydibenzene is electrochemically converted to its radical–anion, the latter decomposes via carbon–oxygen bond cleavage to afford phenoxide (which accepts a proton from the medium to form phenol) and the phenyl radical (which is further reduced and protonated to give benzene). However, for the bulk electrolyses described in the next section, we did not detect benzene, phenol, 1,2-dihydroxybenzene, or any other product that might be derived from the reduction of 2-phenoxyphenol.

3.2. Controlled-potential electrolyses of triclosan

A series of controlled-potential (bulk) electrolyses of triclosan at reticulated vitreous carbon cathodes in DMF – 0.10 M $TBABF_4$ was conducted. Table 1 provides a compilation of the coulometric *n* values and product distributions for experiments done with three different concentrations of triclosan and at three different potentials. Each entry in the table represents the average of three independent experiments. For all of the electrolyses, substantial amounts of tri-*n*-butylamine, formed via an anion-promoted Hofmann elimination that is a signature for the intermediacy of electrogenerated carbanions, were detected but not quantitated.

For the first set of experiments, we chose to hold the cathode potential at −1.65 V, a value corresponding to the valley between the first and second cathodic peaks for the reduction of triclosan (Fig. 1, curve A). For these electrolyses, we observed that the *n* value decreases as the initial concentration of triclosan is raised. Some unreduced triclosan remained at the conclusion of each electrolysis, and the only reduction product was 5-chloro-2-(4-chlorophenoxy)phenol.

Using a cathode potential of −1.82 V (which corresponds to the plateau for the second cathodic wave), we conducted bulk electrolyses of 5.0, 10.0, and 20.0 mM solutions of triclosan at reticulated vitreous carbon electrodes in DMF – 0.10 M $TBABF_4$. At this more negative potential, we again saw that the *n* value decreases as the initial concentration of triclosan increases. Unreduced triclosan was recovered from the electrolysed solutions; as reduction products, we found primarily 5-chloro-2-(4-chlorophenoxy)phenol and

Table 1
Coulometric data and product distributions for direct reduction of triclosan at reticulated vitreous carbon cathodes in DMF containing 0.10 M $TBABF_4$.

Initial concentration of **1** (mM)	*E* (V)	*n*[a]	Product distribution (%)				
			1	**5**	**6**	**7**	Total
5.0	−1.65	1.29	23	58	ND[b]	ND	81
10.0	−1.65	1.21	13	61	ND	ND	74
20.0	−1.65	0.90	18	62	ND	ND	80
5.0	−1.82	2.11	16	60	7	ND	83
10.0	−1.82	1.55	10	65	TR[c]	ND	76
20.0	−1.82	1.39	6	73	TR	ND	79
5.0	−2.10	2.18	16	49	22	TR	87
10.0	−2.10	2.02	8	50	18	TR	76
20.0	−2.10	1.10	23	57	1	ND	81

1 = unreduced triclosan; **5** = 5-chloro-2-(4-chlorophenoxy)phenol; **6** = 5-chloro-2-phenoxyphenol; **7** = 2-phenoxyphenol.
[a] Average number of electrons per molecule of triclosan.
[b] ND = not detected.
[c] TR = trace detected.

only low yields of 5-chloro-2-phenoxyphenol, along with tri-*n*-butylamine.

Finally, at an electrolysis potential of −2.10 V (which corresponds to the plateau for the third cathodic wave), the same trend in *n* value with respect to triclosan concentration was found. Significant amounts of triclosan remained unreduced, and the electrolysis products included 5-chloro-2-(4-chlorophenoxy)phenol and 5-chloro-2-phenoxyphenol, as well as traces of 2-phenoxyphenol, and tri-*n*-butylamine was also detected.

There are several unanticipated and perplexing features of the results listed in Table 1. First, there is no obvious trend in the product distributions as a function of cathode potential; in particular, the extent of reductive dechlorination of triclosan does not increase greatly when electrolyses are done at more negative potentials. Second, the total recovery of starting material and products is significantly below 100%, ranging only from 74% to 87%. Third, the correlation between the experimental coulometric *n* values and the product distributions is imperfect; as an example, for the electrolysis of 20.0 mM triclosan at −1.65 V, the experimental *n* value is 0.90, whereas the production of 5-chloro-2-(4-chlorophenoxy)phenol in 62% yield (a two-electron process) should correspond to 1.24 electrons. All of these findings are atypical of those commonly encountered in most previous investigations in our laboratory. A careful search for other products was conducted with the aid of both GC–MS and LC–MS techniques, but no species other than those shown in Table 1 were detected. Our observation that the *n* value decreases with increasing initial concentration of triclosan suggests the possibility of adsorption of starting material or electrolysis products onto the reticulated vitreous carbon working electrodes, thereby inhibiting the passage of current; however, after an electrolysis, treatment of a working electrode with dichloromethane, followed by analysis of the extract, provided no evidence for the presence of surface-adsorbed compounds. In an earlier study carried out in our laboratory [35], it was found that, at sufficiently negative potentials, $TBABF_4$ can undergo direct reduction at a reticulated vitreous carbon cathode in DMF to afford mixtures of butane, 1-butene, and tri-*n*-butylamine; such a process could contribute to the unexpected *n* values in Table 1. To understand better the behavior of triclosan, we plan to investigate the electrochemistry of several related compounds and to report our findings in future publications.

3.3. Mechanistic picture for the direct reduction of triclosan

On the basis of our electrochemical experiments and the theoretical calculations described below, we propose that the direct reduction of triclosan proceeds according to the mechanistic steps shown in Scheme 1. This sequence of electron-transfer processes and accompanying chemical reactions follows the classic mechanism for the reduction of aryl halides that has been extensively investigated by Savéant and co-workers [36,37].

In Reaction (1), triclosan (**1**) accepts one electron in a reversible process to give a transient aryl radical–anion (**2**). As revealed in Reaction (2), radical–anion **2** loses a chloride ion, followed by uptake of another electron, to form anion **3**, which can exist, in principle, as species **A**, **B**, or **C**. However, as discussed in the following section dealing with theoretical calculations, **A** is more stable than either **B** or **C**. Moreover, on the basis of our theoretical analysis, we propose that anion **A** undergoes a spontaneous intramolecular proton transfer to afford a more stable anion (**A′**), as shown in Reaction (3). Next, anion 4 (as either **A** or **A′**) is protonated by the medium to afford 5-chloro-2-(4-chlorophenoxy)phenol (**5**) (Reaction (4)). Although **5** could conceivably arise through a reaction that involves abstraction of a hydrogen atom from DMF by the aryl radical arising from loss of chloride ion from radical–anion **2**, we regard this process as unimportant due to the facts that the production of **5** is a two-electron process and that tri-*n*-butylamine (formed via a Hofmann elimination involving the supporting electrolyte and electrogenerated carbanions) is a prominent by-product of the reduction of **1**. In Reactions (5) and (6) we show, in abbreviated form, the reduction of **5** to give 5-chloro-2-phenoxyphenol (**6**) and then the final reduction of **6** to yield 2-phenoxyphenol (**7**).

3.4. Theoretical calculations pertaining to the direct reduction of triclosan

To understand the electronic structures of triclosan and the likely products formed from its electrochemical reduction and to provide substantiation for the mechanism proposed in Scheme 1, we performed theoretical studies using density functional theory with the standard B3LYP functional (the three-parameter exchange functional of Becke [38], together with the correlation functional of Lee, Yang, and Parr [39]). A 6-31+G(*d*,*p*) basis set [40,41], containing polarization functions (*d* for C, O, and Cl, and *p* for H) as well as diffuse functions (*sp* for C, O, and Cl), was used to optimize the geometries of the three possible anionic intermediates (carbanions) formed from the removal of each of the three chlorine atoms in triclosan. Single-point calculations were then carried out with a larger 6-311++G(3*df*,2*p*) basis set [42,43] [triple-zeta + diffuse functions (*sp* functions on C, O, and Cl, and *s* functions on H), + multiple polarization functions (3*d*,1*f* on C, O, and Cl and 2*p* on H)] to get more reliable relative energies. Solvation

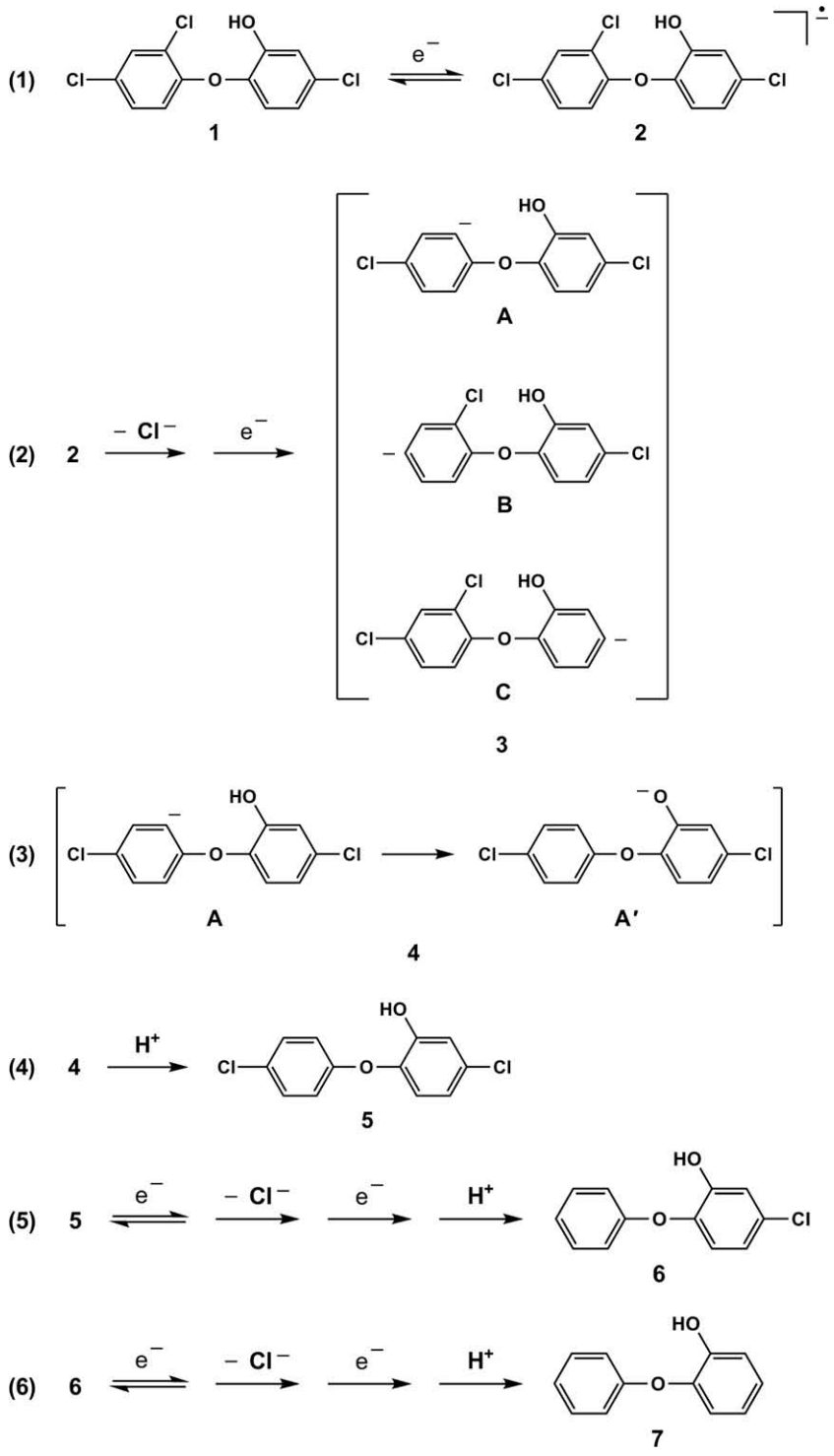

Scheme 1.

effects were included in these larger basis set calculations by a continuum solvation model (Integral Equation Formalism, Polarizable Continuum Model denoted as IEF–PCM) [44,45] based on the use of 36.7 as the dielectric constant for DMF. All calculations were carried out with the Gaussian suite of electronic structure programs [46].

First, let us discuss briefly the structure of the neutral triclosan molecule. It has an optimized geometry with a nearly perpendicular orientation of the two phenyl groups as shown in Fig. 2. This picture is consistent with expectations of preferred ring orientations that are based on simple steric arguments. Notice that the hydrogen of the hydroxy group has a *cis* orientation, and that the hydroxy group points toward the ethereal oxygen and in the general direction of the *ortho* chlorine of the other phenyl moiety.

According to the mechanism proposed in Scheme 1, a carbanion intermediate (**4**) leads, upon protonation, to the observed product **5**. However, there are three possible dichloro monoanionic intermediates that can be formed via two-electron reductive cleavage

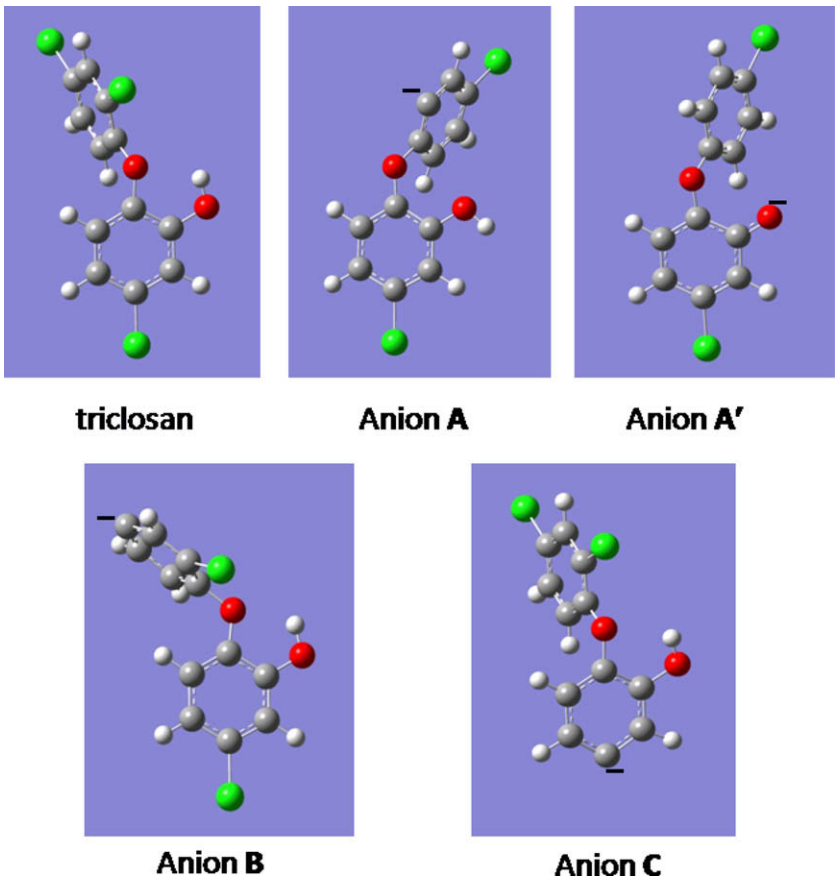

Fig. 2. Optimized geometries for triclosan and for three possible dichloro monoanionic intermediates (**A**, **B**, and **C**) that could be formed via two-electron reductive cleavage of each carbon–chlorine bond of triclosan. Note that **A** undergoes a spontaneous, novel intramolecular proton transfer to form **A′**. See text for further discussion.

of each of the three different chlorine atoms of triclosan. Thus, we focused our attention on these three anions to see if the most likely candidate is consistent with the proposed intermediate, **4**. Fully optimized calculated structures of the three different anions are shown as intermediates **A**, **B**, and **C** in Scheme 1 and Fig. 2, where **A** arises via removal of the *ortho* chlorine of the phenoxy group, **B** arises via removal of the *para* chlorine of the phenoxy group, and **C** arises via removal of the chlorine atom of the phenolic group. Specifically, **A** is the most stable form of the anion that, upon protonation, leads to the dominant product observed experimentally. Although this picture is fully consistent with our results, we noticed a novel intramolecular proton transfer that plays a key role in enhancing the stability of **A**. As our initial structure for **A**, we proposed a carbanion where the negative charge is located at the *ortho* carbon of the phenoxy group (as shown in Scheme 1). However, the proton of the hydroxyl group migrated spontaneously (without any activation barrier) to the carbanion to yield a delocalized phenoxide structure (intermediate **A′** in Scheme 1 and Fig. 2) that is substantially more stable than the other two intermediates (**B** and **C**); indeed **A′** is more stable than **B** by 205 kJ mol^{-1} and more stable than **C** by 222 kJ mol^{-1}. Clearly, the origin of this unusual stability of the resonance-stabilized phenoxide **A′** results from this spontaneous proton migration. We were able to confirm this picture by preventing the migration of the proton by starting from a *trans* orientation of the hydroxide group with respect to the carbanion site. This led to the species labeled **A** in Scheme 1 and Fig. 2 that has an intact carbanion. Anion **A** is more stable than **B**, but by only 25 kJ mol^{-1}. Incorporation of solvation effects on the basis of the IEF–PCM model as well as explicit inclusion of the electrolyte cation (tetra-*n*-butylammonium ion) does not change this qualitative picture. Thus, formation of the major product **5**, as observed experimentally, is fully consistent with the calculated stability of anion **4**, as discussed in Scheme 1, although the actual calculated structure, **A′**, is quite unexpected.

Of the other two carbanions, **B** is more stable than **C** by about 16.7 kJ mol^{-1}. This result is consistent with the larger stabilizing effect of the anion by the hydroxyl group as compared to a chlorine substituent. This finding suggests that, upon further reduction of triclosan, the expected product is 5-chloro-2-phenoxyphenol (**6**), as shown in Scheme 1. Finally, when the third chlorine atom is removed by subsequent reduction, 2-phenoxyphenol (**7**) is formed.

3.5. Catalytic reduction of triclosan by electrogenerated nickel(I) species

We explored the ability of electrogenerated nickel(I) species to catalyze the reduction of triclosan by recording cyclic voltammograms at a scan rate of 100 mV s^{-1} for systems consisting of 5.0 mM triclosan in DMF – 0.10 M $TBABF_4$ in the presence of either 2.0 mM nickel(II) salen or 2.0 mM nickel(II) diethylsalen.

Fig. 3, curve A, shows a cyclic voltammogram for the reversible nickel(II) salen–nickel(I) salen couple; the cathodic peak potential (E_{pc}) and anodic peak potential (E_{pa}) are −0.93 and −0.85 V, respectively. These values, which pertain to DMF – 0.10 M $TBABF_4$, are in good agreement with those reported in a previous investigation by Gosden et al. [47]. When triclosan is introduced into the system, the cathodic peak current (I_{pc}) is larger, whereas the anodic peak current (I_{pa}) diminishes but does not disappear, as revealed by curve B of Fig. 3. Thus, on the time scale of these cyclic voltammetry experiments, electrogenerated nickel(I) salen reacts slowly with triclosan, but not at a sufficiently rapid rate for use as a catalyst. Further evidence that electrogenerated nickel(I) salen is a poor

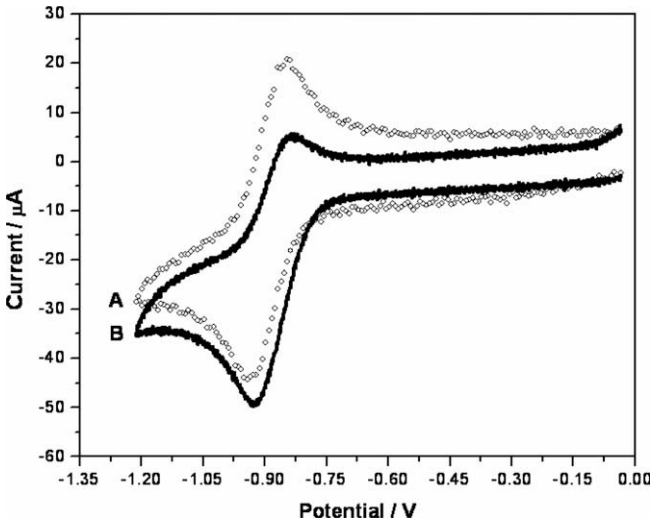

Fig. 3. Cyclic voltammograms recorded at a scan rate of 100 mV s^{-1} with a freshly polished glassy carbon electrode (area = 0.071 cm^2) in oxygen-free DMF containing 0.10 M $TBABF_4$: (A) 2.0 mM nickel(II) salen; (B) 2.0 mM nickel(II) salen and 5.0 mM triclosan. Scans go from 0 to −1.20 to 0 V.

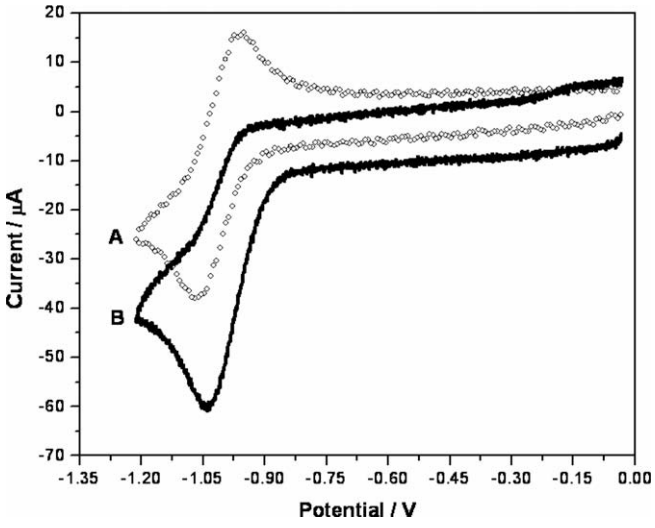

Fig. 4. Cyclic voltammograms recorded at a scan rate of 100 mV s^{-1} with a freshly polished glassy carbon electrode (area = 0.071 cm^2) in oxygen-free DMF containing 0.10 M $TBABF_4$: (A) 2.0 mM nickel(II) diethylsalen; (B) 2.0 mM nickel(II) diethylsalen and 5.0 mM triclosan. Scans go from 0 to −1.20 to 0 V.

agent for the catalytic reduction of triclosan is seen by the fact that the cathodic peak potential (E_{pc}) shifts very little toward positive values—compare the cathodic peak potentials for curves A and B in Fig. 3. Nevertheless, we carried out bulk electrolyses at −1.00 V of a solution containing 2.0 mM nickel(II) salen and 5.0, 10.0, and 20.0 mM triclosan in DMF – 0.10 M $TBABF_4$. Disappointingly, very little of the triclosan was catalytically reduced, and just a small quantity of 5-chloro-2-(4-chlorophenoxy)phenol was detected as a product.

Depicted in Fig. 4, curve A is a cyclic voltammogram recorded at 100 mV s^{-1} for the reversible nickel(II) diethylsalen–nickel(I) diethylsalen redox couple in DMF – 0.10 M $TBABF_4$. One of the effects of the ethyl moieties on the ligand is to shift the cathodic and anodic peak potentials by approximately 100 mV toward more negative values, in comparison with the simpler nickel(II) salen system; thus, for the nickel(II) diethylsalen species, E_{pc} = −1.06 V and E_{pa} = −0.96 V. This negative shift in the peak potentials is sufficient to enhance the reactivity of electrogenerated nickel(I) diethylsalen toward triclosan. Indeed, as shown in curve B of Fig. 4, the presence of 5.0 mM triclosan causes a greater increase in the cathodic peak current, I_{pc}, for reduction of nickel(II) diethylsalen than for nickel(II) salen, and there is no anodic peak. Moreover, a comparison of the cathodic peak potentials for curves A and B of Fig. 4 reveals that the nickel(I) diethylsalen–triclosan reaction causes a measurable positive shift in E_{pc}. Accordingly, we were interested in seeing whether electrogenerated nickel(I) diethylsalen would be a viable catalyst for the reduction of triclosan in a bulk electrolysis. Using a solution containing 5.0 mM triclosan and 2.0 mM nickel(II) diethylsalen in DMF – 0.10 M $TBABF_4$, we carried out duplicate electrolyses at −1.00 V. On the basis of gas chromatographic peak areas, the ratio of unreduced triclosan to 5-chloro-2-(4-chlorophenoxy)phenol was 11:1. Obviously, the reaction between triclosan and either of the electrogenerated nickel(I) species is too slow to be of value.

Acknowledgments

High-resolution mass analyses were performed in the Indiana University Mass Spectrometry Facility; the HRMS system was purchased with funds provided by the National Institutes of Health Grant No. 1S10RR016657-01.

References

[1] R.M. Pemberton, J.P. Hart, Anal. Chim. Acta 390 (1999) 107.
[2] A. Safavi, N. Maleki, H.R. Shahbaazi, Anal. Chim. Acta 494 (2003) 225.
[3] A. Safavi, N. Maleki, H.R. Shahbaazi, Bull. Electrochem. 21 (2005) 229.
[4] L.-H. Wang, S.-C. Chu, C.-Y. Chin, Bull. Electrochem. 20 (2004) 225.
[5] J. Wang, J. Farrell, Environ. Sci. Technol. 38 (2004) 5232.
[6] M.A. Ghanem, R.G. Compton, B.A. Coles, E. Psillakis, M.A. Kulandainathan, F. Marken, Electrochim. Acta 53 (2007) 1092.
[7] P. Raghupathy, J. Mathiyarasu, J. Joseph, K.L.N. Phani, V. Yegnaraman, J. Electroanal. Chem. 584 (2005) 210.
[8] I. Sirés, N. Oturan, M.A. Oturan, R.M. Rodríguez, J.A. Garrido, E. Brillas, Electrochim. Acta 52 (2007) 5493.
[9] M. Amiri, S. Shahrokhian, E. Psillakis, F. Marken, Anal. Chim. Acta 593 (2007) 117.
[10] M.J. Bonne, K.J. Edler, J.G. Buchanan, D. Wolverson, E. Psillakis, M. Helton, W. Thielemans, F. Marken, J. Phys. Chem. C 112 (2008) 2660.
[11] L. Vidal, A. Chisvert, A. Canals, E. Psillakis, A. Lapkin, F. Acosta, K.J. Edler, J.A. Holdaway, F. Marken, Anal. Chim. Acta 616 (2008) 28.
[12] C. Saby, K.B. Male, J.H.T. Luong, Anal. Chem. 69 (1997) 4324.
[13] J.D. Rodgers, W. Jedral, N.J. Bunce, Environ. Sci. Technol. 33 (1999) 1453.
[14] Z. Ežerskis, Z. Jusys, Chemija 11 (2000) 155.
[15] H. Cheng, K. Scott, P.A. Christensen, J. Electrochem. Soc. 150 (2003) D17.
[16] H. Cheng, K. Scott, P.A. Christensen, J. Electrochem. Soc. 150 (2003) D25.
[17] H. Wang, J. Wang, Electrochim. Acta 53 (2008) 6402.
[18] J.D. Persinger, J.L. Hayes, L.J. Klein, D.G. Peters, J.A. Karty, J.P. Reilly, J. Electroanal. Chem. 568 (2004) 157.
[19] M.S. Mubarak, P.C. Gach, D.G. Peters, Electroanalysis 18 (2006) 417.
[20] P.C. Gach, M.S. Mubarak, J.A. Karty, D.G. Peters, J. Electrochem. Soc. 154 (2007) F1.
[21] G.W. Bishop, J.A. Karty, D.G. Peters, J. Electrochem. Soc. 154 (2007) F65.
[22] P.C. Gach, J.A. Karty, D.G. Peters, J. Electroanal. Chem. 612 (2008) 22.
[23] K.L. Vieira, D.G. Peters, J. Electroanal. Chem. 196 (1985) 93.
[24] P. Vanalabhpatana, D.G. Peters, J. Electrochem. Soc. 152 (2005) E222.
[25] J.A. Cleary, M.S. Mubarak, K.L. Vieira, M.R. Anderson, D.G. Peters, J. Electroanal. Chem. 198 (1986) 107.
[26] L.W. Marple, Anal. Chem. 39 (1967) 844.
[27] C.W. Manning, W.C. Purdy, Anal. Chim. Acta 51 (1970) 124.
[28] J.L. Hall, P.W. Jennings, Anal. Chem. 48 (1976) 2026.
[29] W.A. Pritts, K.L. Vieira, D.G. Peters, Anal. Chem. 65 (1993) 2145.
[30] A. Di Teodoro, W. Hölzl, D. Reinehr, R. Zink, US Patent 6,596,907 (2000).
[31] C. Gosden, K.P. Healy, D. Pletcher, J. Chem. Soc., Dalton Trans. (1978) 972.
[32] L.J. Klein, K.S. Alleman, D.G. Peters, J.A. Karty, J.P. Reilly, J. Electroanal. Chem. 481 (2000) 24.
[33] M.D. Koppang, N.F. Woolsey, D.E. Bartak, J. Am. Chem. Soc. 107 (1985) 4692.
[34] T.A. Thornton, N.F. Woolsey, D.E. Bartak, J. Am. Chem. Soc. 108 (1986) 6497.
[35] C.E. Dahm, D.G. Peters, J. Electroanal. Chem. 402 (1996) 91.
[36] C.P. Andrieux, C. Blocman, J.-M. Dumas-Bouchiat, J.-M. Savéant, J. Am. Chem. Soc. 101 (1979) 3431.
[37] C.P. Andrieux, J.-M. Savéant, K.B. Su, J. Phys. Chem. 90 (1986) 3815.
[38] A.D. Becke, J. Chem. Phys. 98 (1993) 5648.
[39] C.T. Lee, W.T. Yang, R.G. Parr, Phys. Rev. B 37 (1988) 785.
[40] P.C. Hariharan, J.A. Pople, Theor. Chim. Acta 28 (1973) 213.

[41] M.M. Francl, W.J. Petro, W.J. Hehre, J.S. Binkley, M.S. Gordon, D.J. DeFrees, J.A. Pople, J. Chem. Phys. 77 (1982) 3654.
[42] R. Krishnan, J.S. Binkley, R. Seeger, J.A. Pople, J. Chem. Phys. 72 (1980) 650.
[43] J.-P. Blaudeau, M.P. McGrath, L.A. Curtiss, L. Radom, J. Chem. Phys. 107 (1997) 5016.
[44] B. Mennucci, E. Cancès, J. Tomasi, J. Phys. Chem. B 101 (1997) 10506.
[45] E. Cancès, B. Mennucci, J. Chem. Phys. 114 (2001) 4744.
[46] M.J. Frisch, G.W. Trucks, H.B. Schlegel, G.E. Scuseria, M.A. Robb, J.R. Cheeseman, J.A. Montgomery Jr., T. Vreven, G. Scalmani, B. Mennucci, V. Barone, G.A. Petersson, M. Caricato, H. Nakatsuji, M. Hada, M. Ehara, K. Toyota, R. Fukuda, J. Hasegawa, M. Ishida, T. Nakajima, Y. Honda, O. Kitao, H. Nakai, X. Li, H.P. Hratchian, J.E. Peralta, A.F. Izmaylov, K.N. Kudin, J.J. Heyd, E. Brothers, V.N. Staroverov, G. Zheng, R. Kobayashi, J. Normand, J.L. Sonnenberg, F. Ogliaro, M. Bearpark, P.V. Parandekar, G.A. Ferguson, N.J. Mayhall, S.S. Iyengar, J. Tomasi, M. Cossi, N. Rega, J.C. Burant, J.M. Millam, M. Klene, J.E. Knox, J.B. Cross, V. Bakken, C. Adamo, J. Jaramillo, R. Gomperts, R.E. Stratmann, O. Yazyev, A.J. Austin, R. Cammi, C. Pomelli, J.W. Ochterski, P.Y. Ayala, K. Morokuma, G.A. Voth, P. Salvador, J.J. Dannenberg, V.G. Zakrzewski, S. Dapprich, A.D. Daniels, M.C. Strain, O. Farkas, D.K. Malick, A.D. Rabuck, K. Raghavachari, J.B. Foresman, J.V. Ortiz, Q. Cui, A.G. Baboul, S. Clifford, J. Cioslowski, B.B. Stefanov, G. Liu, A. Liashenko, P. Piskorz, I. Komaromi, R.L. Martin, D.J. Fox, T. Keith, M.A. Al-Laham, C.Y. Peng, A. Nanayakkara, M. Challacombe, W. Chen, M.W. Wong, J.A. Pople, Gaussian Development Version, Revision G.01, Wallingford, CT, USA, 2007.
[47] C. Gosden, J.B. Kerr, D. Pletcher, R. Rosas, J. Electroanal. Chem. 117 (1981) 101.